RADIATION RESEARCH **169**, 214–222 (2008)
0033-7587/08 $15.00

Biochemical Kinetics Model of DSB Repair and Induction of γ-H2AX Foci by Non-homologous End Joining

Francis A. Cucinotta,[a,1] Janice M. Pluth,[b] Jennifer A. Anderson,[c] Jane V. Harper[c] and Peter O'Neill[c]

[a] *NASA, Lyndon B. Johnson Space Center, Houston, Texas 77058;* [b] *Lawrence Berkeley National Laboratory, Life Sciences Division, Berkeley, California 94720; and* [c] *DNA Damage Group, Radiation and Genome Stability Unit, Medical Research Council, Harwell, Didcot, Oxfordshire, OX11 0RD, United Kingdom*

Cucinotta, F. A., Pluth, J. M., Anderson, J. A., Harper, J. V. and O'Neill, P. Biochemical Kinetics Model of DSB Repair and Induction of γ-H2AX Foci by Non-homologous End Joining. *Radiat. Res.* 169, 214–222 (2008).

We developed a biochemical kinetics approach to describe the repair of double-strand breaks (DSBs) produced by low-LET radiation by modeling molecular events associated with non-homologous end joining (NHEJ). A system of coupled nonlinear ordinary differential equations describes the induction of DSBs and activation pathways for major NHEJ components including Ku70/80, DNA-PKcs, and the ligase IV-XRCC4 heterodimer. The autophosphorylation of DNA-PKcs and subsequent induction of γ-H2AX foci observed after ionizing radiation exposure were modeled. A two-step model of regulation of repair by DNA-PKcs was developed with an initial step allowing access of other NHEJ components to breaks and a second step limiting access to ligase IV-XRCC4. Our model assumes that the transition from the first to the second step depends on DSB complexity, with a much slower rate for complex DSBs. The model faithfully reproduced several experimental data sets, including DSB rejoining as measured by pulsed-field gel electrophoresis (PFGE) at 10 min postirradiation or longer and quantification of the induction of γ-H2AX foci. A process that is independent of DNA-PKcs is required for the model to reproduce experimental data for rejoining before 10 min postirradiation. Predictions are made for the behaviors of NHEJ components at low doses and dose rates, and a steady state is found at dose rates of 0.1 Gy/h or lower.

INTRODUCTION

A mechanistic description of the processing of DNA double-strand breaks (DSBs) is important for the understanding of ionizing radiation effects leading to cell death, mutation, genomic instability, and carcinogenesis. Mathematical models of DSB repair are important for the description of radiation modalities not accessible by experimental means and for their possible predictive capabilities. Past mathematical models of ionizing radiation-induced DSB repair have relied largely on phenonemological approaches that did not consider specific molecular interactions involved in DSB repair (*1–3*). Previously, we showed that a biochemical approach based on nonlinear kinetics has some special features for describing DSB repair, including the time delay caused by a DSB-repair enzyme intermediate complex (*3*). Application of biochemical kinetics models to describe experimental data on DSB repair at the molecular level is a goal of the present study.

Non-homologous end joining (NHEJ) is the primary pathway for DSB repair in eukaryotic cells (*4–6*), and defects in NHEJ increase radiation sensitivity and the risk of carcinogenesis (*7, 8*). Many of the steps involved in NHEJ have been characterized experimentally, including the initial recognition of DSBs by the Ku70/80 heterodimer, subsequent recruitment of the DNA-dependent protein kinase catalytic subunit (DNA-PKcs), and formation of the DNA-dependent protein kinase (DNA-PK) (*6–9*). DNA-PKcs contains several serine-threonine residues that are autophosphorylated. Autophosphorylation of various subsets of these sites is thought to be important in regulating the choice between NHEJ or homologous recombination repair (HR) (*6*). In addition to DNA-PKcs, a number of other proteins have been implicated as being important in either NHEJ or HR. For example, Artemis in conjunction with both ATM and DNA-PKcs has been suggested to function in DNA end processing of specific, difficult-to-repair, radiation-induced damages (*10–13*), and both ligase IV and XRCC4 have been shown to be important in the ligation step of NHEJ (*14, 15*).

DNA-PKcs is a member of the phosphoinositide 3 kinase-related protein kinase (PIKK) family, which includes the ataxia telangiectasia mutated (ATM) and ataxia telangiectasia and Rad3-related (ATR) proteins, and these proteins play a role in sensing DNA damage (*5*). In addition to damage sensing, both ATM and ATR have been shown to have roles distinct from those of DNA-PKcs, consisting of G_1/S, S and G_2/M cell cycle checkpoint regulation (*5, 16*) and replication stress response (*19*), respectively. DNA-

[1] Address for correspondence: NASA, Lyndon B. Johnson Space Center, 2101 NASA Parkway, Houston TX 77058; e-mail: Francis.A.Cucinotta@nasa.gov.

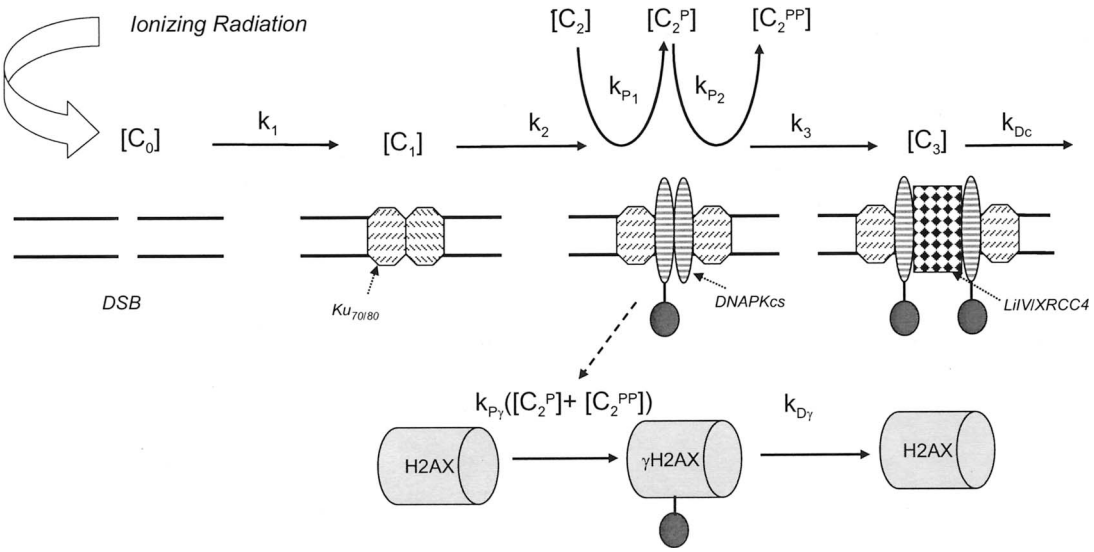

FIG. 1. Schematic of biochemical kinetics model of DSB repair by NHEJ with induction of γ-H2AX by DNA-PKcs. The key components of the model and associated rate constants are shown. Not illustrated is the degradation of the $[C_3]$ complex after the ligation step or the distinction between simple and complex DSBs including the formation of residual DSBs when complex initial DSBs do not proceed to the $[C_2^{PP}]$ complex.

PKcs, ATM and ATR share common features including a conserved carboxy-terminal motif (*5*) and a reliance on upstream activators, Ku70/80, the MRE-Rad50-Nbs1 complex (MRN), and ATRIP, respectively. ATR is believed to function largely in S phase, whereas DNA-PKcs and ATM have important roles throughout the cell cycle (*16–19*). The activation step of DNA-PKcs and ATM is rapid, occurring in a few minutes to about 30 min (*5, 9, 18*). Both activated proteins have been shown to lead to the phosphorylation of the histone variant H2AX in a chromatin region corresponding to about 2 Mbp around the DSB, with the phosphorylated form denoted as γ-H2AX (*20, 21*). Total numbers of γ-H2AX foci have been shown to be fairly representative of the total number of DSBs (*20, 22, 23*). In addition, a correlation between loss of γ-H2AX foci and radiation sensitivity has been noted (*23–25*).

The plethora of experimental studies involving NHEJ repair should facilitate the development of mathematical models of these processes. In this paper we have developed a systems biology approach to NHEJ repair that can be used to make predictions for other radiation modalities, including extrapolations to low doses and dose rates. Systems biology seeks to describe emergent properties of biological systems from the interactions of molecules acting in specific pathways (*26*). We use this approach to describe DSB rejoining curves and the kinetics of the formation and loss of γ-H2AX to gain insights into the kinetics of the NHEJ repair pathway. A key component of a biochemical kinetics model is the role of DNA repair complex intermediates, which leads naturally to a nonlinear description of kinetics (*3*). We consider several intermediate complexes based on data on γ-H2AX radiation-induced repair foci and experimental studies of DNA-PKcs and relate their description to DSB rejoining curves determined by pulsed-field gel electrophoresis (PFGE).

Ionizing radiation produces DSBs that vary from simple to complex structures and are produced in the same proportions with increasing dose but depend on radiation quality (*27, 28*). Clustered DNA damage sites are defined as two or more elemental lesions within one or two helical turns of DNA produced by a single radiation track (*27, 29*). Under this definition, all DSBs are clustered damage sites; however, complex DSBs are defined by the presence of other damage types, such as base damage, damaged ends, single-strand breaks near a DSB, or two or more DSBs in proximity. Clustered non-DSB damage can lead to secondary DSBs produced during damage processing (*30, 31*). For low-LET radiation, it has been estimated that 20–40% of the initial damage is complex (*27–29*). Closely spaced multiple DSBs could inhibit the attachment of repair proteins to other nearby DSBs, and this possibility increases with the ionization density or linear energy transfer (LET) of the radiation. We hypothesize that processing of complex DSBs involves additional NHEJ factors including the Artemis (*10–13*), MRN (*19*) and ATM proteins (*10*).

METHODS

DNA-PK Regulation and Repair Complexes

We use the mass-action chemical kinetics approach to describe the binding of repair enzymes to DSBs with several intermediate repair complexes leading to DNA rejoining: (1) an initial complex bound by the Ku70/80 heterodimer, (2) Ku-mediated DNA-PKcs binding, (3) the regulation of the DSB-DNA-PKcs complex through autophosphorylation by DNA-PK, and (4) a final repair complex involving the Ligase IV/XRCC4 heterodimer, denoted *LiIV*. Figure 1 is a schematic diagram of our model showing the sequence of proteins binding to the repair complex and the

two activation steps considered; phosphorylation of DNA-PKcs and H2AX. The series of repair complexes are denoted C_j or with the superscript P for autophosphorylation in complex, e.g. C_j^P. The first complex (C_1) is formed by Ku70/80 binding to the DSB, the second through binding by DNA-PKcs to the first complex forming C_2, etc., through to the final ligation step. Because these proteins are post-transcriptionally regulated, the total number of enzymes in free form or complex form is assumed to be conserved.

DSBs are assumed to be induced per unit dose rate with an efficiency of α (Gy^{-1} per cell). The Ku70/80 heterodimer is highly abundant and rapidly attaches to the DSB (denoted as C_0), leading to the mass-action equation,

$$\frac{d[C_0]}{dt} = \alpha\frac{dD}{dt} - k_1\text{Ku70/80}[C_0], \tag{1}$$

forming the repair complex, C_1, which is followed quickly by DNA-PKcs binding,

$$\frac{d[C_1]}{dt} = k_1[C_0]\text{Ku70/80} - k_2[DNAPKcs][C_1], \tag{2}$$

to form a second complex, C_2. Equations (1) and (2) follow the convention that symbols within brackets define, for a given molecular species, the time-dependent number of copies per cell. The repair complex, C_2, is then modified by phosphorylation events that facilitate cleaning of the ends, signal transduction, and the translation of DNA-PKcs away from the ends of the break to allow ligation. Autophosphorylation of a cluster of residues on DNA-PKcs, denoted ABCDE, is expected to be a gatekeeper that regulates access to the break by other repair proteins (*6*). The phosphorylation of a second cluster of residues on DNA-PKcs, denoted PQR, has been suggested to promote HR (*6*), whereas phosphorylation of the ABCDE cluster is thought to inhibit HR (*6*). The PQR cluster has been noted to partially facilitate dissociation of DNA-PK from the ends; however, it is expected that other phosphorylation sites are needed for complete disassembly (*6*). To date, phosphorylation of Ku70/80 has not been implicated as being critical for the actual repair of DSBs (*32*) and thus will not be considered in the model.

We consider a two-step model that depicts the role of DNA-PKcs in the regulation of repair involving activation events controlled by autophosphorylation of DNA-PKcs. The exact nature of the autophosphorylation of DNA-PKcs is not known (*6, 33, 34*). Autophosphorylation may occur in *trans*, where one DNA-PKcs molecule phosphorylates a second molecule on opposing sides of a DSB, a second-order reaction. Alternatively, it may occur in *cis*, by an intramolecular mechanism, a first-order reaction. Both of these mechanisms may occur and could depend on the DSB end structure (*32, 33*). We have modeled the autophosphorylation of DNA-PKcs bound to the DSB ends as first-order for both steps in regulation of repair of DNA-PKcs. We assume the second step depends on the complexity of the DSB and may involve other proteins, including Artemis and other poorly defined repair proteins. Residual breaks are predicted to arise at complex DSB sites through a competing first-order process that assumes that not all complex DSBs are successfully rejoined, with the failure occurring before the transition to the ligation step of the reaction. The resulting equations are

$$\frac{d[C_2]}{dt} = k_2[DNAPKcs][C_1] - k_{P_1}[C_2]; \tag{3}$$

$$\frac{d[C_2^P]}{dt} = k_{P_1}[C_2] - k_{P_2}[C_2^P] - k_{res}[C_2^P]; \tag{4}$$

$$\frac{d[C_2^{PP}]}{dt} = k_{P_2}[C_2^P] - k_3[LiIV][C_2^{PP}]; \tag{5}$$

$$\frac{d[DSB_{res}]}{dt} = k_{res}[C_2^P]. \tag{6}$$

The rates k_{P2} and k_3 are assumed to depend on the complexity of the DSB, and k_{res} is set to zero for simple DSBs.

The last step in our model involves ligation of the ends by the ligase IV/XRCC4 complex, denoted *LiIV*, and enzyme release given by

$$\frac{d[C_3]}{dt} = k_3[LiIV][C_2^{PP}] - k_{D_c}[C_3]. \tag{7}$$

The ligase IV/XRCC4 complex is also regulated by covalent modifications (*13*), but this observation is not currently treated in our model.

Kinetics of γ-H2AX Foci

The histone variant H2AX is phosphorylated after DNA damage by each of the family of PIK3 phospho-proteins ATM, ATR and DNA-PKcs (*5*). In the G_1 phase of the cell cycle, ATM and DNA-PKcs phosphorylate H2AX with nearly equal rates and in an overlapping manner (*35*). γ-H2AX foci appear at a distance from DSBs corresponding to a region of 2 Mbp (*20*), and it is not known how many H2AX molecules are modified per DSB or what mechanism leads to phosphorylation of a large number of H2AX molecules surrounding the break. We use Michaelis-Menten kinetics to describe the rate of induction of H2AX by DNA-PKcs in its active forms as given by

$$\frac{d[\gamma\text{-H2AX}]}{dt} = \frac{k_{P\gamma}[C_{\text{DNA-PKcs}}][\text{H2AX}]}{K_M + [C_{\text{DNA-PKcs}}]} - k_{D\gamma}[\gamma\text{-H2AX}], \tag{8}$$

where $[C_{\text{DNA-PKcs}}]$ is the sum of active forms of DNA-PKcs (C_2^P, C_2^{PP} and C_3). The mechanism of dephosphorylation of γ-H2AX foci has not been well studied. We assume this step follows a simple first-order decay law in Eq. (8).

Scaling Variables

To simplify the model solutions, we introduce new scaled variables by considering the conservation relationships for the total concentration of a given protein and noting that the sum of all repair complexes is equal to the initial number of DSBs. The new scaled variables are introduced using the definitions,

$$H_i = [E_i] + \sum_{j=i}^{n}[C_j] = \text{const.};$$

$$h_i(t) = \frac{\sum_{j=i}^{n}[C_j]}{H_i}; \qquad \kappa_i = H_i k_i \quad \text{and}$$

$$c_i(t) = \frac{[C_i]}{H_1},$$

which after substitution leads to the system of equations

$$\frac{dc_0(t)}{dt} = \frac{\alpha}{H_1}\frac{dD}{dt} - \kappa_1 c_0(t)[1 - h_1(t)]; \tag{9}$$

$$\frac{dc_1(t)}{dt} = \kappa_1 c_0(t)[1 - h_1(t)] - \kappa_2 c_1(t)[1 - h_2(t)]; \tag{10}$$

$$\frac{dc_2(t)}{dt} = \kappa_2 c_1(t)[1 - h_2(t)] - k_{P_1}c_2(t); \tag{11}$$

$$\frac{dc_2^P(t)}{dt} = k_{P_1}c_2(t) - (k_{P_2} + k_{res})c_2^P(t); \tag{12}$$

$$\frac{dc_2^{PP}(t)}{dt} = k_{P_2}c_2^P(t) - \kappa_3 c_2^{PP}(t)[1 - h_3(t)]; \tag{13}$$

$$\frac{dc_{res}(t)}{dt} = k_{res}c_2^P(t); \tag{14}$$

$$\frac{dc_3(t)}{dt} = \kappa_3 c_2^{PP}(t)[1 - h_3(t)] - k_{D_c}c_3(t). \tag{15}$$

All rate constants are assumed to be independent of the type of initial

DSB, except for k_{P2} and κ_3, which are given distinct values for simple and complex DSBs, respectively. For the solutions in terms of the scaled variables, only the value of H_1 enters since all other H_i are combined with the k_i to form the rate parameters, κ_i, which are in units of h^{-1}. The functions $h_i(t)$ include contributions from repair complexes involving both simple and complex DSBs.

The histone variant H2AX content varies with cell lineage, representing from 2 to 10% of all nucleosomes, and there are about 2.0×10^6 H2AX molecules per cell (*20*). We reasoned that it was more useful to model the kinetics of the number of γ-H2AX foci formed rather than the number of activated molecules. For focus-counting experiments, the number of foci is limited by the model-dependent initial number of DSBs per cell. For low-LET radiation, the probability of more than one DSB within the spatial region of foci is small; however, for high-LET radiation, other considerations will need to be taken into account (Cucinotta *et al.*, in preparation). Assuming that [γ-H2AX] + [H2AX] is constant and denoting $\gamma(t)$ as the time-dependent number of foci leads to

$$\frac{d\gamma(t)}{dt} = \frac{\kappa_{P_\gamma} c_{\text{DNA-PKcs}}(t)[1 - \gamma(t)]}{\kappa_M + c_{\text{DNA-PKcs}}(t)} - k_{D_\gamma}\gamma(t), \tag{16}$$

where $\kappa_{P\gamma} = k_{P\gamma}/H_1$. For comparison to DSB rejoining kinetics in an acute irradiation measured using PFGE, the number of DSBs remaining is given by

$$DSB_{\text{remaining}}(t) = H_1\left[\sum_{j=0}^{3} c_j(t) + c_{res}(t)\right]. \tag{17}$$

For comparison to experimental data on relative Ku70/80 induction, which includes Ku70/80 in various DSB repair complexes, the following sum is used:

$$C_{\text{Ku70/80}}(t) = H_1 \sum_{j=1}^{3} c_j(t). \tag{18}$$

The equations formulated above to represent NHEJ are nonlinear ordinary differential equations, described as stiff equations, which are equations where the values for the various parameters, k_i or κ_i, vary over several orders of magnitude. These equations were solved numerically using the method of backward difference approximates. We note that the factors "$1 - h_i$" in our scaled equation have values close to unity at low doses where the initial number of DSB is $\ll H_1$.

RESULTS AND DISCUSSION

Our kinetics model of NHEJ consists of a system of eight coupled nonlinear ordinary differential equations for each class of DSBs (simple and complex). This system of equations describe major components in the NHEJ repair pathway and the phosphorylation of H2AX by DNA-PKcs. Values for rate constants were determined by comparing to experimental data with cell lineage-specific values estimated for rate constants and other parameters as listed in Table 1. Our scaling approach results in a significant reduction in parameter space since it avoids the need to estimate values for the total cellular concentrations of Ku70/80, DNA-PKcs, *LiIV* and XRCC4, which are effectively replaced by a single constant, H_1. The value of H_1 can be interpreted as the total number of copies of Ku70/80. However, in the model, other constants, H_j, could be used as the scaling variable, and we prefer to interpret the value of H_1 as the total number of DNA repair complexes that could occur in a cell (*3*). We have fixed this value at a large number ($H_1 = 3000$) to ensure that the shape of the DSB rejoining curve is largely independent of dose over the range from 1 to 40 Gy. To reduce the number of variable parameters, we fixed the peak time of the $[C_1]$ complex, corresponding to the binding of Ku70/80 to DSBs, at about 1 min postirradiation (*36*), and of the $[C_2]$ complex, corresponding to the binding of DNA-PKcs complex, at about 3 min for all cell lineages considered using the values for κ_1 and κ_2 as listed in Table 1. The remaining parameters are determined in a cell lineage-specific manner by comparing the model solutions to data for DSB rejoining and the induction and loss of γ-H2AX foci. *In vitro* assays provide insights into kinetic rates for DNA-PKcs activation through autophosphorylation and show typical times from a few minutes to 30 min (*33, 37, 38*), which lends support for our values of autophosphorylation for simple DSBs.

TABLE 1
Values of Rate Constants and other Parameters in the Biochemical Model[a,b]

Rate constant	V79 cells	HF19 cells	T98G cells
α, Gy^{-1}	16	25	25
κ_3, h^{-1}	8 (0.5)	8 (0.5)	8 (0.5)
k_{P1}, h^{-1}	10	10	10
k_{P2}, h^{-1}	10 (0.5)	10 (0.5)	10 (0.5)
$\kappa_{P\gamma}$, $copy^{-1}\ h^{-1}$	1000	900	1000
k_{Dc}, h^{-1}	4	4	2
$k_{D\gamma}$, h^{-1}	2	2	0.75
κ_M	0.5	0.5	0.5
k_{res}, h^{-1}	0 (0.05)	0 (0.05)	0 (0.05)

Note. Values in parentheses are used for complex DSB repair.

[a] Values of κ_1, κ_2, and H_i are set at 100 h^{-1}, 100 h^{-1}, and 3000 per cell for all cell lineages considered. Values chosen correspond to a peak for a DSB-$Ku_{70/80}$ complex at about 1 min postirradiation (*36*) and assuming a peak of DSB-$Ku_{70/80}$-DNA-PK_{cs} complex at about 3 min postirradiation.

[b] The initial number of breaks per Gy (α) determined from experiments reported in refs. (*23*, *29*). We use the same values for GM5738 cells and HF19 cells.

Figure 2 illustrates the model predictions for the time evolution of the sequence of repair complexes formed after an acute dose of 1 Gy for simple and complex damage processing. The value of C_3 exceeds that of C_2^P and C_2^{PP} up to ~1 h postirradiation but then drops to lower values of C_2^P and C_2^{PP} at longer times, when only the slower complex DSBs remain, since a portion of these breaks are defined as residual breaks as described by Eqs. (4) and (6) when they remain unrepaired.

We compared our model to the rejoining kinetics determined by PFGE, which is available in the literature for X rays. DSB rejoining kinetics measured by PFGE was determined at high doses (>10 Gy) and must be corrected for the presence of heat-labile sites (*30, 39, 40*), which results in artifactual DSBs and can account for up to 50% of the fragment yields at early postirradiation times (within 30 min postirradiation). To avoid the contribution of heat-labile sites, we compared the PFGE data of Stenerlow *et al.* (*40*), analyzed using the cold lysis method developed by Rydberg (*39*), to the data for GM5758 diploid fibroblasts

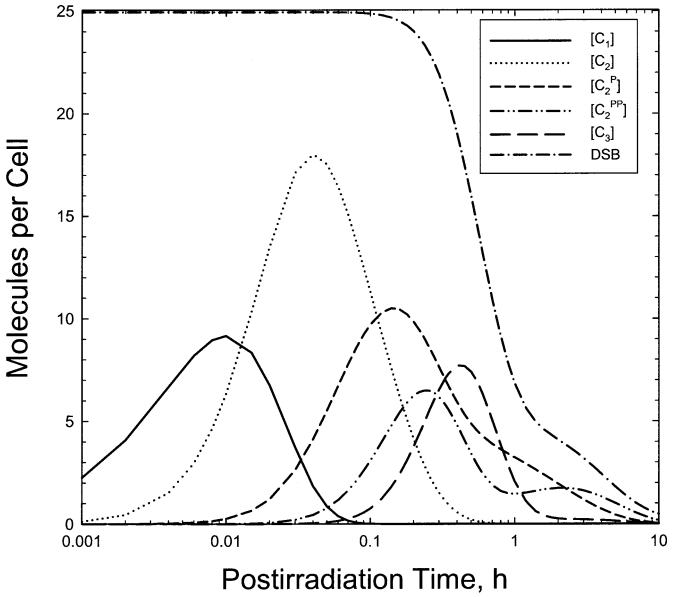

FIG. 2. Model calculations of time course for sequence of DNA repair complexes in NHEJ pathway and DSB rejoining curve (non-complex only) for 1 Gy γ rays in normal human diploid fibroblast cells.

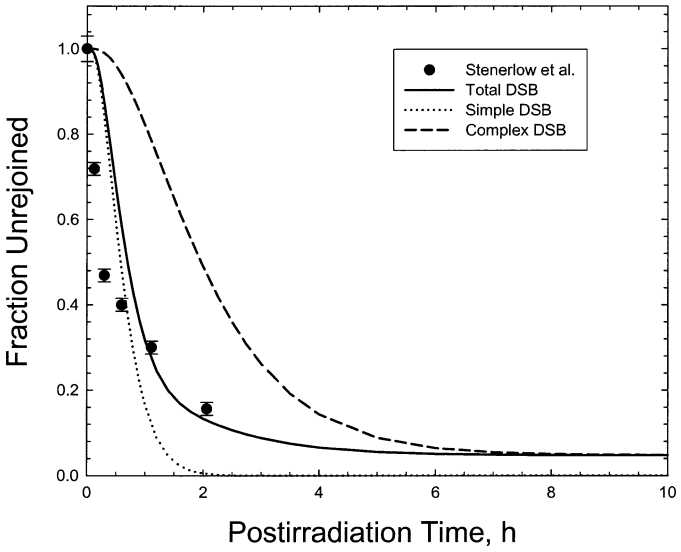

FIG. 3. Comparisons of model calculations to data for DSB rejoining determined by PFGE for GM5758 human diploid fibroblasts at 40 Gy (*40*). The solid line shows the contributions from simple and complex DSBs. For comparison we show calculations of the rejoining curves for simple and complex DSBs in our model normalized to unity.

as shown in Fig. 3. We used the experimentally determined values of Gulston *et al.* (*23*) for HF19 cells for the value of α, the total number of DSBs per Gy, of 25 as initial conditions, and assumed that 20% of the initial breaks are repaired, requiring additional processing steps between the transition from C_2^P to C_2^{PP} and hence slower kinetic parameters.

At moderate doses (<5 Gy) the model predicts a lack of rejoining in the first 10–15 min postirradiation as the multiple steps in NHEJ proceed. The persistence of DSBs for the initial 10-15 min has been shown to occur in V79-4 cells once the rapid repair of heat-labile sites has occurred within 4 min (*30*). Furthermore, some DSBs may be rejoined by direct ligation independent of DNA-PKcs (*36*), leading to a faster repair component at early times, beyond those contributed by heat-labile sites. We have considered an alternative model (results not shown) that allows for a small component of initial DSBs (<20%) that rejoin independent of DNA-PKcs. Such a model provides an improved fit at earlier times but introduces several new rate constants and does not influence any of our findings at the later times, which are expected to be more biologically relevant.

Track structure calculations provide some estimates of the fractions of simple and complex DSB lesions. However, the mechanisms that would be available to repair the differential spectrum of DSBs produced by ionizing radiation are not well understood and may use additional factors, including Artemis (*10–13*), ATM (*10*), MRN (*19, 41*), and Werner syndrome (*42*) proteins, and perhaps components in the nucleotide or base excision repair pathways. In our model we assume just two average components corresponding to so-called broad categories, namely simple and complex DSBs.

The fraction of residual DSBs is easily modeled when the complex DSBs are considered if one assumes that a first-order process results near the end of the cascade described above. We used a first-order rate constant for residual breaks at 0.05 h^{-1}, assuming that a small fraction of the initial complex DSBs remain unrepaired at the C_2^P complex and lead to residual DSBs. The model presented here thus provides a framework to describe the dependence of residual breaks on radiation quality, dose rate and postirradiation time.

We compared our model to data for the time courses and dose response for γ-H2AX foci. Using confocal microscopy, Leatherbarrow *et al.* (*23*) measured the number of γ-H2AX foci in V79 and HF19 cells. We found good agreement with their results, as shown in Fig. 4a and b. If focus size increases at early times postirradiation, it will influence the number of foci counted, perhaps leading to an underestimate if the size is below detection levels. Costes *et al.* (*43*) found no dependence on focus size with postirradiation time up to 2 h for low-LET radiation. For high-LET nitrogen ions, focus size was dynamic, increasing with postirradiation time (*43*). Comparisons of the number of γ-H2AX foci at 0.5 and 4 h postirradiation made by Short *et al.* (*44*) are shown in Fig. 5. The inset in Fig. 5 shows our results at low doses for focus components above the background. Focus induction is predicted to be linear in this region.

Our biochemical model can be used to study the correlation between the counting of γ-H2AX or other repair protein foci with the initial number of DSBs produced by ionizing radiation. Figure 6 shows this correlation for several

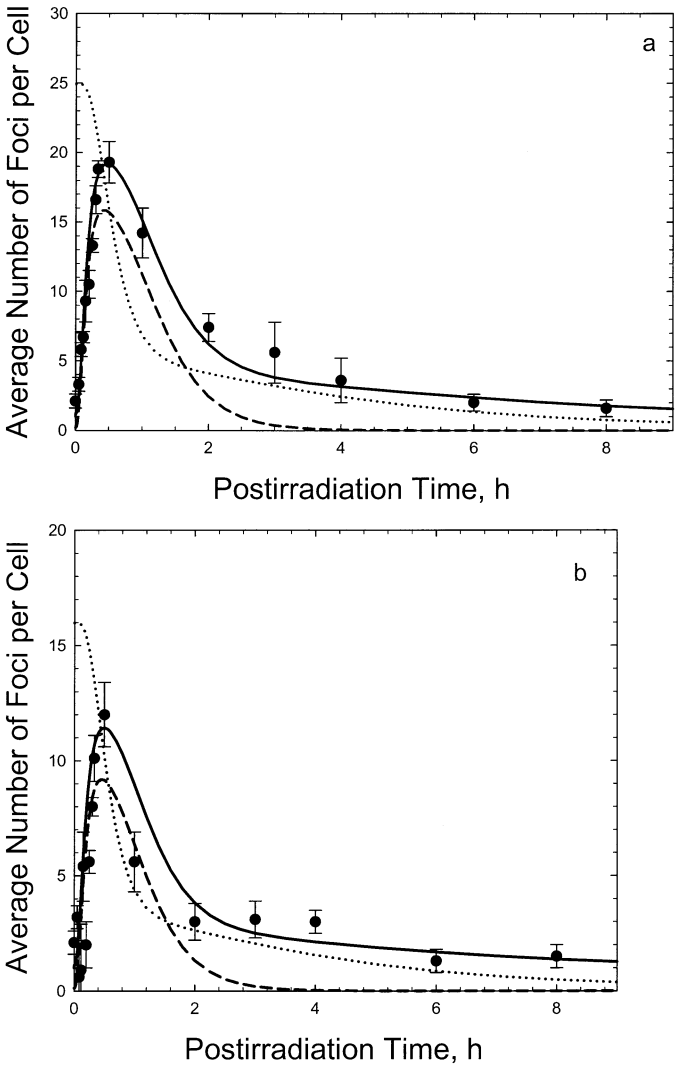

FIG. 4. Comparisons of model calculations to measurements of γ-H2AX foci by Leatherbarrow *et al.* (*23*). Solid line, total (simple and complex DSBs) induced γ-H2AX foci; dashed line, foci from simple DSBs alone; dotted line, the number of DSBs remaining. Symbols with error bars are the experimental results (*23*). Panel a: HF19 cells at 1 Gy; panel b: V79 cells at 1 Gy.

postirradiation times and shows that the number of γ-H2AX foci under-represents the true number of foci for low-LET radiation by ~20% at the optimal time of about 30 min postirradiation. There is a concomitant induction of γ-H2AX from active ATM (*35*) monomers, which was studied in the current model. ATM and DNA-PKcs are expected to induce these foci with similar efficiencies (*35*); however, the inclusion of ATM will likely modify our predictions and will need to be studied.

The understanding of dose-rate effects is an important consideration in radiation protection, especially for low-LET radiation (*45, 46*). Since the processing of DSBs after irradiation is a determinant in mutation, chromosome aberrations, and carcinogenesis, we studied the induction of various NHEJ components as a function of varying dose rates and doses. Steady-state solutions for the systems equations can be found when focus counts become independent of dose rate. The results shown in Fig. 7 predict that the number of DSB repair complexes per cell seen as γ-H2AX foci becomes independent of dose for dose rates below about 0.1 Gy/h. These observations can be tested with experiments. Also, our description of NHEJ can be

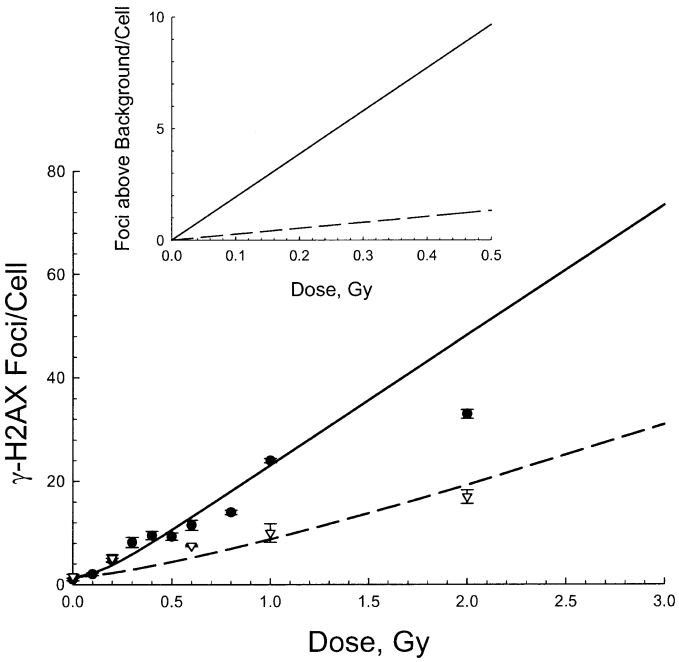

FIG. 5. Comparisons of model calculations for dose response for γ-H2AX foci at 0.5 (closed circles) and 4 h (open triangles) postirradiation using data of Short *et al.* (*44*). Model calculations shown are solid line at 0.5 h and dashed line at 4 h postirradiation. The inset shows model predictions for doses below 0.5 Gy for focus levels above the background.

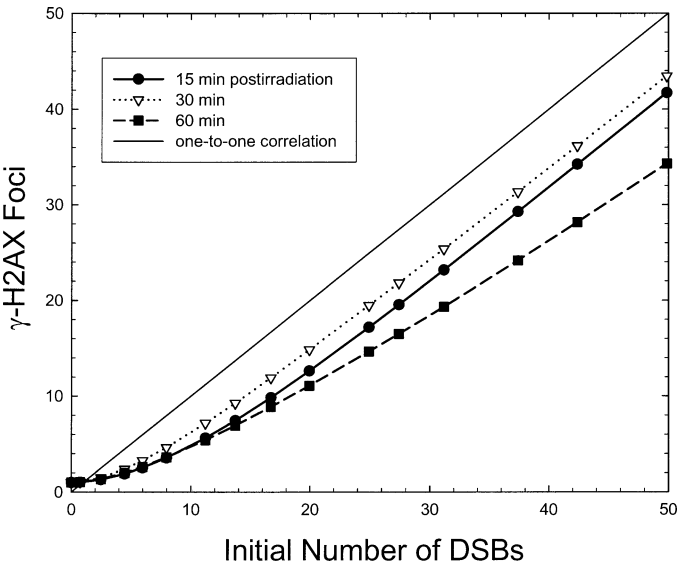

FIG. 6. Biochemical correlation between the number of initial DSBs and γ-H2AX foci observed at several postirradiation times illustrating the defect in the observed number of foci and the initial number of DSBs due to the biochemical steps occurring in focus formation and removal. A background of one focus per cell is assumed.

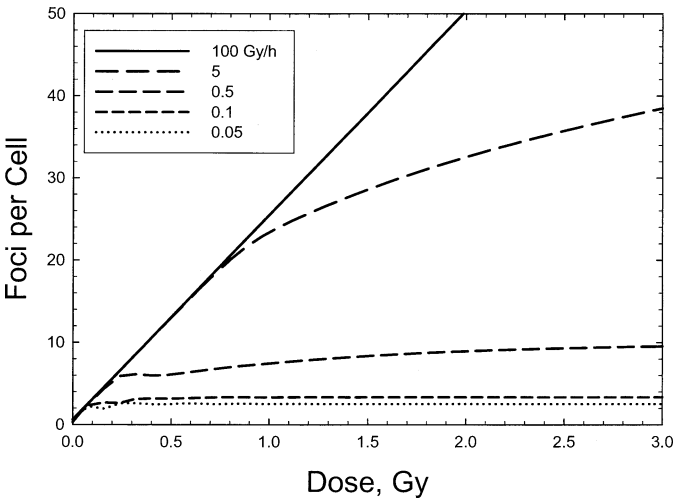

FIG. 7. Predictions for the number of DSB repair complexes as a function of dose for various dose rates in human fibroblasts.

used as a starting point for building mechanistic models of mutation and chromosomal aberrations. In addition, studying dose-rate dependences for repair should be informative in understanding dose-rate effects for these other end points.

Several improvements to our model are planned to develop a complete systems biology model of NHEJ. We plan to describe the induction of γ-H2AX foci by ATM upon its activation and localization to DSB as dependent on the MRN complex (*5, 18, 19*). ATM and DNA-PK lead to similar numbers of γ-H2AX foci (*35, 47*); however, distinct downstream substrates are involved, and it will be important to describe these aspects in our model. We expect that the inclusion of the multiple mechanisms of activation of H2AX by ATM and DNA-PKcs in our model could lead to a time-dependent description of focus size at early times postirradiation.

The results presented here are based on a first-order decay model for the loss of γ-H2AX foci. We considered several alternative approaches, including ones where the loss of γ-H2AX foci occurred only after ligation of the DSB. Here we allowed the decay term for γ-H2AX to be dependent on the C_3 complex of Eq. (7). The results were similar to those reported here, but they required specification of additional and largely underdetermined rate constants. We plan to use new information emerging on the phosphatases responsible for the dephosphorylation of γ-H2AX and possible relationships to chromatin dynamics and checkpoint recovery (*48–50*) in future work. Such data should allow us to improve the description of the loss of γ-H2AX. We have introduced two classes of DSBs, with the slower-rejoining class dependent on additional steps by DNA-PK. We expect in future work to model misrepair leading to mutation or chromosomal aberrations as originating from this slower-rejoining class of DSBs. It will be important to describe the additional factors such as Artemis and ATM in the processing steps for complex DSBs and to investigate possible correlations between processing of the slower-rejoining DSBs with mutation and the dephosphorylation of γ-H2AX. Such considerations will be especially important for high-LET radiation, where a larger proportion of complex DSBs occur (*23, 27, 51*).

In summary, we have synthesized a large number of experimental observations into a biochemical kinetic model of the NHEJ repair pathway. The model is based on the current mechanistic understanding of the molecular binding and kinase activity of major NHEJ components that have been described experimentally. The model is capable of describing the time courses and dose and dose-rate dependences for major NHEJ components, the induction of γ-H2AX foci upon activation of DNA-PKcs through autophosphorylation, and DSB rejoining kinetics as measured by PFGE. The model presented here can be modified as more information about the molecular mechanisms of NHEJ repair is obtained. The ability to describe the kinetics of DSB induction and repair and the various associated protein complexes will support models of chromosomal aberrations as a function of radiation quality when descriptions of DSB complexity and spatial dependence of initial DSBs are coupled to the present model (*27, 28, 51*). We plan to extend our work to include theoretical descriptions of the fractions of simple and complex initial DSBs for high-LET radiation and the resulting changes in DSB repair kinetics and to include the description of the ATM signaling pathway in our model.

ACKNOWLEDGMENTS

We gratefully acknowledge partial financial support provided by the U.S. DOE (DE-FG02-05ER64090 and DE-A103-05ER64088) and NASA (03-OBPR-07-0032-0027).

Received: March 21, 2007; accepted: September 7, 2007

REFERENCES

1. D. T. Goodhead, Saturable repair models of radiation action in mammalian cells. *Radiat. Res.* **104** (Suppl.), S58–S67 (1985).
2. J. Kiefer, A repair fixation model based on classical enzyme kinetics. In *Quantitative Models in Radiation Biology* (J. Kiefer, Ed.), pp. 171–180. Springer-Verlag, Berlin, 1988.
3. F. A. Cucinotta, H. Nikjoo, P. O'Neill and D. T. Goodhead, Kinetics of DSB rejoining and formation of simple chromosome exchange aberrations. *Int. J. Radiat. Biol.* **76**, 1463–1474 (2000).
4. S. P. Lees-Miller and K. Meek, Repair of DNA double strand breaks by non-homologous end-joining. *Biochemie* **85**, 1161–1173 (2003).
5. J. Falck, J. Coates and S. P. Jackson, Conserved modes of recruitment of ATM, ATR, and DNA-PK$_{cs}$ to sites of DNA damage. *Nature* **434**, 605–611 (2005).
6. X. Cui, Y. Yu, S. Gupta, Y. M. Cho, S. Lees-Miller and K. Meek, Autophosphorylation of DNA-dependent protein kinase regulates DNA end processing and may also alter double-strand break repair choice. *Mol. Cell Biol.* **25**, 10842–10652 (2005).
7. D. O. Ferguson, J. M. Sekiguchi, S. Chang, K. M. Frank, Y. Gao, R. A. DePinho and F. W. Alt, The nonhomologous end-joining pathway of DNA repair is required for genomic instability and the suppression of translocations. *Proc. Natl. Acad. Sci. USA* **97**, 6630–6633 (2000).

8. M. Martin, A. Genesca, L. Lutre, I. Jaco, G. E. Taccioli, J. Egozcue, M. A. Blasco, G. Iliakis and L. Tusell, Post-replicative joining of DNA double strand breaks causes genomic instability in DNA-PK_{cs}-deficient mouse embryonic fibroblasts. *Cancer Res.* **65**, 10223–10232 (2005).
9. D. W. Chan, B. P. Chen, S. Prithivirajsingh, A. Kurimasa, M. D. Story, J. Qin and D. J. Chen, Autophosphorylation of the DNA-dependent protein kinase catalytic subunit is required for rejoining of DNA double strand breaks. *Genes Dev.* **16**, 2333–2338 (2002).
10. J. Drouet, P. Frit, C. Delteil, J. P. de Villartay, B. Salles and P. Calsou, Interplay between Ku, Artemis, and the DNA-dependent protein kinase catalytic subunit at DNA ends. *J. Biol. Chem.* **281**, 27784–27793 (2006).
11. P. Jeggo and P. O'Neill, The Greek Goddess, Artemis, reveals the secrets of her cleavage. *DNA Repair* **1**, 771–777 (2002).
12. J. Wang, J. M. Pluth, P. K. Cooper, M. J. Cowan, D. J. Chen and S. M. Yannone, Artemis phosphorylation and function in response to damage. *DNA Repair* **4**, 556–570 (2005).
13. E. Riballo, M. Kuhne, N. Rief, A. Doherty, G. C. Smith, M. J. Recio, C. Reis, K. Dahm, A. Fricke and M. Löbrich, A pathway of double-strand break rejoining dependent upon ATM, Artemis and proteins locating to γ-H2AX foci. *Mol. Cell* **16**, 715–724 (2004).
14. H. Wang, Z. C. Zeng, A. R. Perrault, X. Cheng, W. Qin and G. Iliakis, Genetic evidence for the involvement of DNA Ligase IV in the DNA-PK-dependent pathway of non-homologous end joining in mammalian cells. *Nucleic Acids Res.* **29**, 1653–1660 (2001).
15. J. Drouet, C. Delteil, J. Lefrancois, P. Concannon, B. Salles and P. Calsou, DNA-dependent protein kinase and XRCC4-DNA Ligase IV mobilization in the cell in response to DNA double strand breaks. *J. Biol. Chem.* **280**, 7060–7069 (2005).
16. K. D. Brown, Y. Ziv, S. N. Sadanandan, L. Chess, F. S. Collins, Y. Shiloh and D. A. Tagle, The ataxia-telangiectasia gene product, a constitutively expressed nuclear protein that is not upregulated following genome damage. *Proc. Natl. Acad. Sci. USA* **94**, 1840–1845 (1997).
17. D. P. Gately, J. C. Hittle, G. K. T. Chan and T. J. Yen, Characterization of ATM expression, localization, and associated DNA-dependent protein kinase activity. *Mol. Biol. Cell* **9**, 2361–2374 (1998).
18. C. J. Bakkenist and M. B. Kastan, DNA damage activates ATM through intermolecular autophosphorylation and dimer dissociation. *Nature* **421**, 499–506 (2003).
19. A. Dupre, L. Boyer-Catenet and J. Gautie, Two-step activation of ATM by DNA and the Mre11-Rad50-Nbs1 complex. *Nat. Struct. Mol. Biol.* **13**, 451–457 (2006).
20. E. P. Rogakou, D. R. Pilch, A. H. Orr, V. S. Ivanova and W. M. Bonner, DNA double-strand breaks induce histone H2AX phosphorylation on serine 139. *J. Biol. Chem.* **273**, 5858–5868 (1998).
21. T. T. Paull, E. P. Rogakou, V. Yamazaki, C. U. Kirchgessner, M. Gellert and W. M. Bonner, A critical role for histone H2AX in recruitment or repair factors to nuclear foci after DNA damage. *Curr. Biol.* **10**, 886–895 (2000).
22. K. Rothkamm and M. Löbrich, Evidence for a lack of DNA double-strand break repair in human cells exposed to very low x-ray doses. *Proc. Natl. Acad. Sci. USA* **100**, 5057–5062 (2003).
23. E. L. Leatherbarrow, J. V. Harper, F. A. Cucinotta and P. O'Neill, Induction and quantification of γ-H2AX foci formation following low- and high-LET radiation. *Int. J. Radiat. Biol.* **82**, 111–118 (2006).
24. P. L. Olive and J. P. Banath, Phosphorylation of histone H2AX as a measure of radiosensitivity. *Int. J. Radiat. Oncol. Biol. Phys.* **58**, 331–335 (2004).
25. J. P. Banath, S. H. MacPhail and P. L. Olive, Radiation sensitivity, H2AX phosphorylation, and kinetics of repair of DNA strand breaks in irradiated cervical cancer cell lines. *Cancer Res.* **64**, 7144–7149 (2004).
26. L. Alberghina and H. V. Westerhoff, Eds., *Systems Biology. Definitions and Perspectives.* Vol. 13 of *Topics in Current Genetics.* Springer-Verlag, Berlin/Heidelberg, 2005.
27. D. T. Goodhead, Initial events in the cellular effects of ionising radiation: clustered damage in DNA. *Int. J. Radiat. Biol.* **65**, 7–17 (1994).
28. H. Nikjoo, P. O'Neill, W. E. Wilson and D. T. Goodhead, Computational approach for determining the spectrum of DNA damage induced by ionizing radiation. *Radiat. Res.* **156**, 577–583 (2001).
29. M. Gulston, J. Fulford, T. Jenner, C. de Lara and P. O'Neill, Clustered DNA damage induced by γ-radiation in human fibroblasts (HF19), hamster (V79-4) cells and plasmid DNA is revealed as Fpg and Nth sensitive sites. *Nucleic Acids Res.* **30**, 3464–3472 (2002).
30. M. Gulston, C. de Lara, T. Jenner, E. Davis and P. O'Neill, Processing of clustered DNA damage generates additional DSB in mammalian cells post-irradiation. *Nucleic Acids. Res.* **32**, 1602–1609 (2004).
31. I. M. Ward and J. Chen, Histone H2AX is phosphorylated in an ATR-dependent manner in response to replicational stress. *J. Biol. Chem.* **276**, 47759–47762 (2001).
32. S. Jin and D. T. Weaver, Double-strand break repair by Ku70 requires heterodimerization with Ku80 and DNA binding functions. *EMBO J.* **16**, 6874–6885 (1997).
33. M. Jovanovic and W. S. Dynan, Terminal DNA structure and ATP influence binding parameters of the DNA-dependent protein kinase at an early step prior to DNA synapsis. *Nucleic Acid Res.* **34**, 1112–1120 (2006).
34. E. Weterings, N. S. Verkaik, H. T. Bruggernwirth, J. H. J. Hoejimakers and D. C. van Gent, The role of DNA dependent protein kinase in synapsis of DNA ends. *Nucleic Acids Res.* **31**, 7238–7246 (2003).
35. T. Stiff, M. O'Driscoll, N. Rief, K. Iwabuhi, M. Löbrich and P. A. Jeggo, ATM and DNA-PK function redundantly to phosphorylate H2AX after exposure to ionizing radiation. *Cancer Res.* **64**, 2390–2396 (2004).
36. P. O. Mari, B. I. Florea, S. P. Persengiev, N. S. Verkaik, H. T. Brüggenwirth, M. Modesti, G. Giglia-Mari, K. Bezstarosti, J. A. Demmers and D. C. van Gent, Dynamic assembly of end-joining complexes requires interaction between Ku70/80 and XRCC4. *Proc. Natl. Acad. Sci. USA* **103**, 18597–18602 (2006).
37. Y. V. R. Reddy, Q. Ding, S. P. Lees-Miller, K. Meek and D. A. Ramsden, Non-homologous end joining requires that the DNA-PK complex undergo an autophosphorylation-dependent rearrangement at DNA ends. *J. Biol. Chem.* **279**, 39408–39413 (2004).
38. W. D. Bloch, Y. Yu, D. Merkle, J. L. Gifford, Q. Ding, K. Meek and S. P. Lees-Miller, Autophosphorylation-dependent remodeling of the DNA-dependent protein kinase catalytic subunit regulated ligation of DNA ends. *Nucleic Acids Res.* **32**, 4351–4357 (2004).
39. B. Rydberg, Radiation-induced heat-labile sites that convert into DNA double-strand breaks. *Radiat. Res.* **153**, 805–12 (2000).
40. B. Stenerlow, K. H. Karlsson, B. Cooper and B. Rydberg, Measurement of prompt DNA double-strand breaks in mammalian cells without inducing heat-labile sites: Results for cells deficient in nonhomologous end joining. *Radiat. Res.* **159**, 502–510 (2003).
41. T. T. Paull, and M. Gilbert, The 3′ to 5′ exonuclease activity of Mre11 facilitates repair of DNA double-strand breaks. *Mol. Cell* **1**, 869–879 (1998).
42. C. von Kobbe, N. H. Thöma, B. K. Czyzewski, N. P. Pavleitch and V. A. Bohr, Werner syndrome protein contains three structure-specific DNA binding domains. *J. Biol. Chem.* **278**, 52997–53006 (2003).
43. S. V. Costes, A. Bossiere, S. Ravani, R. Romano, B. Parvin and M. H. Barcellos-Hoff, Imaging features that discriminate between foci induced by high- and low-LET radiation in human fibroblasts. *Radiat. Res.* **165**, 505–515 (2006).
44. S. C. Short, S. Bourne, C. Martindale, M. Woodcock and S. P. Jackson, DNA damage responses to low radiation doses. *Radiat. Res.* **164**, 292–302 (2005).
45. National Research Council, Committee on Biological Effects of Ionizing Radiation, *Health Risks from Exposure to Low Levels of Ionizing Radiation (BEIR VII).* National Academy Press, Washington, DC, 2005.
46. F. A. Cucinotta and M. Durante, Cancer risk from exposure to ga-

lactic cosmic rays: implications for space exploration by human beings. *Lancet Oncol.* **7**, 431–435 (2006).

47. H. Wang, M. Wang, H. Wang, W. Bocker and G. Iliakis, Complex H2AX phosphorylation patterns by multiple kinases including ATM and DNA-PK in human cells exposed to ionizing radiation and treated with kinase inhibitors. *J. Cell. Physiol.* **202**, 492–502 (2005).

48. D. Chowdhury, M. Keogh, H. Ishii, C. L. Peterson, S. Buratowski and J. Liberman, γ-H2AX dephosphorylation by protein phosphatase 2A facilitates DNA double-strand break repair. *Mol. Cell* **20**, 1–9 (2005).

49. M. C. Keogh, J. A. Kim, M. Downey, J. Fillingham, D. Chowdhury, J. C. Harrison, M. Ohishi, N. Datta, S. Galicia and N. J. Krogan, A phosphatase complex that dephosphorylates γH2AX regulates DNA damage checkpoint recovery. *Nature* **439**, 497–501 (2006).

50. J. A. Downs, M. C. Nussenzweig and A. Nussenzweig, Chromatin dynamics and the preservation of genetic information. *Nature* **447**, 951–958 (2007).

51. A. Ponomarev and F. A. Cucinotta, Chromatin loops are responsible for higher counts of small DNA fragments induced by high-LET radiation, while chromosomal domains do not affect the fragment sizes. *Int. J. Radiat. Biol.* **82**, 293–305 (2006).